Effect of 475 °C Embrittlement on Fractal Behavior and Tensile Properties of a Duplex Stainless Steel

O.A. Hilders, L. Sáenz, M. Ramos, and N.D. Peña

(Submitted 2 July 1998; in revised form 15 September 1998)

The fractal dimension variations of several tension fracture surfaces of a duplex stainless steel broken at room temperature has been studied after several aging treatments performed at 475 °C for 1, 2, 6.5, 12, 24, 40, and 120 h. A dimple type of fracture mode was observed for small aging times and transgranular as well as dimple rupture for 24, 40, and 120 h of aging. The higher the time of aging is, the smaller the fractal dimension and the true fracture strain. An expected reduction of the strength with the time of aging was observed.

Keywords 475 °C embrittlement, fractal dimension, stainless steels

Many studies have been devoted to the subject of fractals since Mandelbrot (Ref l) developed the branch of mathematics called fractal geometry. Fractals are noneuclidean geometrical constructs that can relate rough, irregular, or fragmented surfaces to the phenomena that cause them. Fractals characteristically are self-similar in shape and scale. The scaling structure of a surface is characterized by a number *D* called the fractal dimension. The calculated fractal dimension of a smooth curve equals the euclidean dimension of a line. However, for an irregular line, *D* is greater than 1 and increases with increasing roughness to a limit of 2. For surfaces, *D* can range from 2, for a smooth surface, to 3 for a volume-filling object.

Fractal geometry is a very useful tool for evaluating the geometrical characteristics of a fracture surface (Ref 2-6). Although much of the work on fractal characteristics of metallic alloys has shown a relationship between *D* and toughness (Ref 7-11), no experimental measurement of the fractal dimension-tensile properties relationship is available for many commercial metallic alloys. The present experiments on a duplex stainless steel show that *D* can be used as a characterization parameter because it correlates well with the strength and ductility values derived from tension tests.

On the other hand, due to the very good combination of the most outstanding properties of ferrite and austenite, the microstructure of duplex stainless steels allows them to obtain high strength and toughness levels (even at low temperatures) and good resistance to localized corrosion and stress corrosion cracking (Ref 12-14). As a result of these combined effects, duplex stainless steels have become very popular for many applications in the chemical and oil industries. In practice, the prolonged use of these materials at temperatures below approximately 500 °C may cause an embrittlement of the ferrite phase, which has been called 475 °C embrittlement. The embrittling reaction due to the decomposition of the ferrite phase into a Cr-rich, α', and Fe-rich phase, α, impairs the toughness and enhances the hardness (Ref 15, 16). Thus, the isothermal aging at 475 °C can be exploited to produce a variety of strength values associated with the corresponding decreases in ductility and variations of the fractal dimension of the fracture surfaces.

The composition of the duplex stainless steel employed is listed in Table 1. The as-received material was originally hot rolled to a rod of ≅31 mm diameter by a commercial supplier. The microstructure consisted of elongated domains of ferrite and austenite, the proportion of the phases being approximately 50 to 50. Cylindrical specimens (with reduced section diameters of 6.35 mm and gage lengths of 25.4 mm) for tensile testing were machined from the rods, solution treated for 2 h at 1120 °C, water quenched, and subsequently aged at 475 °C for 1, 2, 6.5, 12, 24, 40, and 120 h (two samples for each condition). Room temperature tensile tests were done by duplicate in an Instron tensile machine (Instron Corporation, Canton, MA) at a strain rate of 10^{-3} s^{-1}. The fracture surfaces of the broken samples were analyzed using a Hitachi S2400 scanning electron microscope (Nissei Sangyo Corp., Tokyo, Japan) operated at 25 kV. One fracture surface for each condition was mounted in resin. Before the mounting step, the fracture surfaces were given an electroless coating, in order to preserve the features of the profiles generated after a cross-sectioning operation perpendicular to the surface.

After metallographic preparation, the profiles were analyzed to evaluate their apparent length, *L*, with a digitizing software using rulers of different sizes, η, according to the fracture profile analysis (Ref 17, 18) and to the Richardson-Mandelbrot equation (Ref 19):

Table 1 Chemical composition of the material

Chemical	Composition, wt %
Cr	21.90
Ni	5.50
Mo	3.10
N	0.13
Mn	1.50
Si	1.13
C	0.03
Fe	bal

O.A. Hilders, M. Ramos, and **N.D. Peña,** School of Metallurgical Engineering and Materials Science, Central University of Venezuela (UCV), Apartado 47514, Caracas, 1041-A Venezuela; **L. Sáenz,** Department of Materials and Fabrication Processes, University of Carabobo (UC), Apartado 3155, Valencia, 2002 Venezuela.

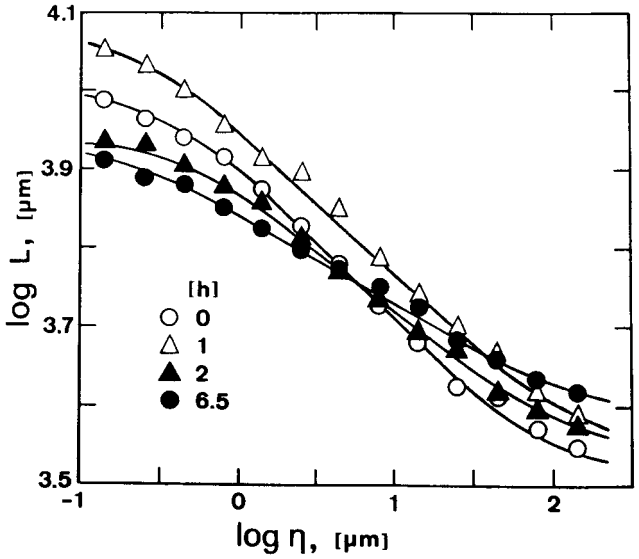

Fig. 1 Richardson-Mandelbrot curves corresponding to the as-received condition and for the material aged at 475 °C between 1 and 6.5 h

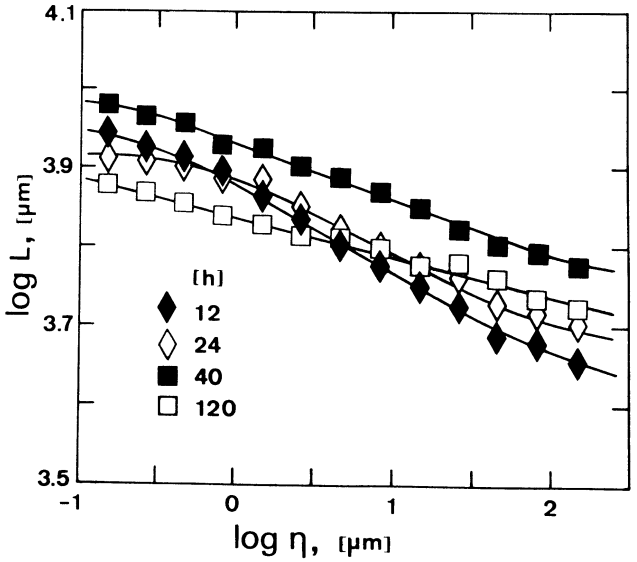

Fig. 2 Richardson-Mandelbrot curves corresponding to the material aged at 475 °C between 12 and 120 h

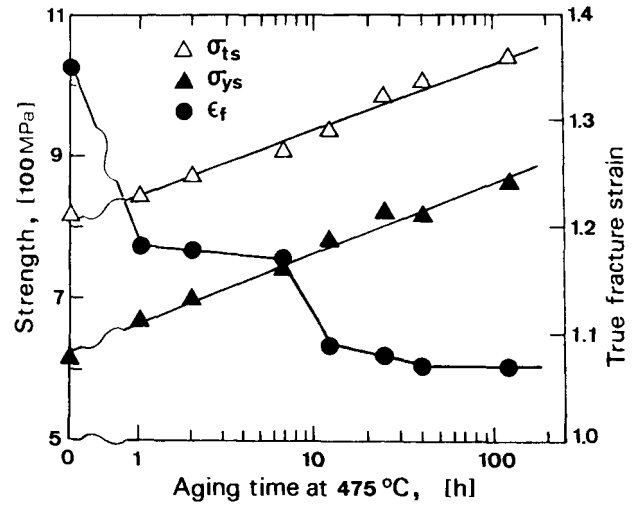

Fig. 3 Effect of aging time on strength and ductility of the duplex stainless steel studied

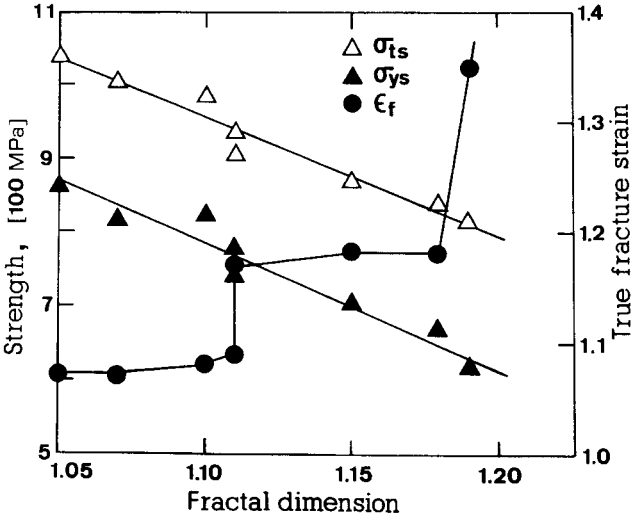

Fig. 4 Dependence of strength and ductility on the fractal dimension of fracture surfaces

$$L(\eta) = L_0 \eta^{-(D-1)}$$

where L_0 is a constant with dimensions of length. Figures 1 and 2 show the inverse relationship between L and the size of the measurement unit η for the as-received condition and for the isothermal aging treatments. In general, the curves from Fig. 1 and 2 show the reversed sigmoidal behavior (Ref 20); then the values of D were evaluated in the central linear portion of each curve. As can be seen in Table 2, the fractal dimension values decrease monotonically with the aging time, from 1.19 for the as-received condition, to 1.05 for the material aged for 120 h.

Figure 3 is a semilogarithmic plot that demonstrates the effect of aging time on yield strength, σ_{ys}, true tensile strength, σ_{ts}, and true fracture strain, ε_f. Aging at 475 °C induced significant embrittlement, which promotes an increase in yield strength and true tensile strength and a decrease in ductility. This is not surprising, because it is well established that the majority of all factors or treatments that strengthen metallic alloys are associated with a decrease in ductility. All these effects are attributed to the precipitation of α', which enhances the tendency to twinning, imposing restrictions on the slip processes and increasing the possibility for microcrack initiation (Ref 21). Figure 4 summarizes the relation developed between the tensile properties and D. Since the fractal dimension has been considered a measure of the surface roughness (Ref 22, 23), the direct relation between D and ε_f displayed in this figure can be explained in terms of the microvoid morphology developed

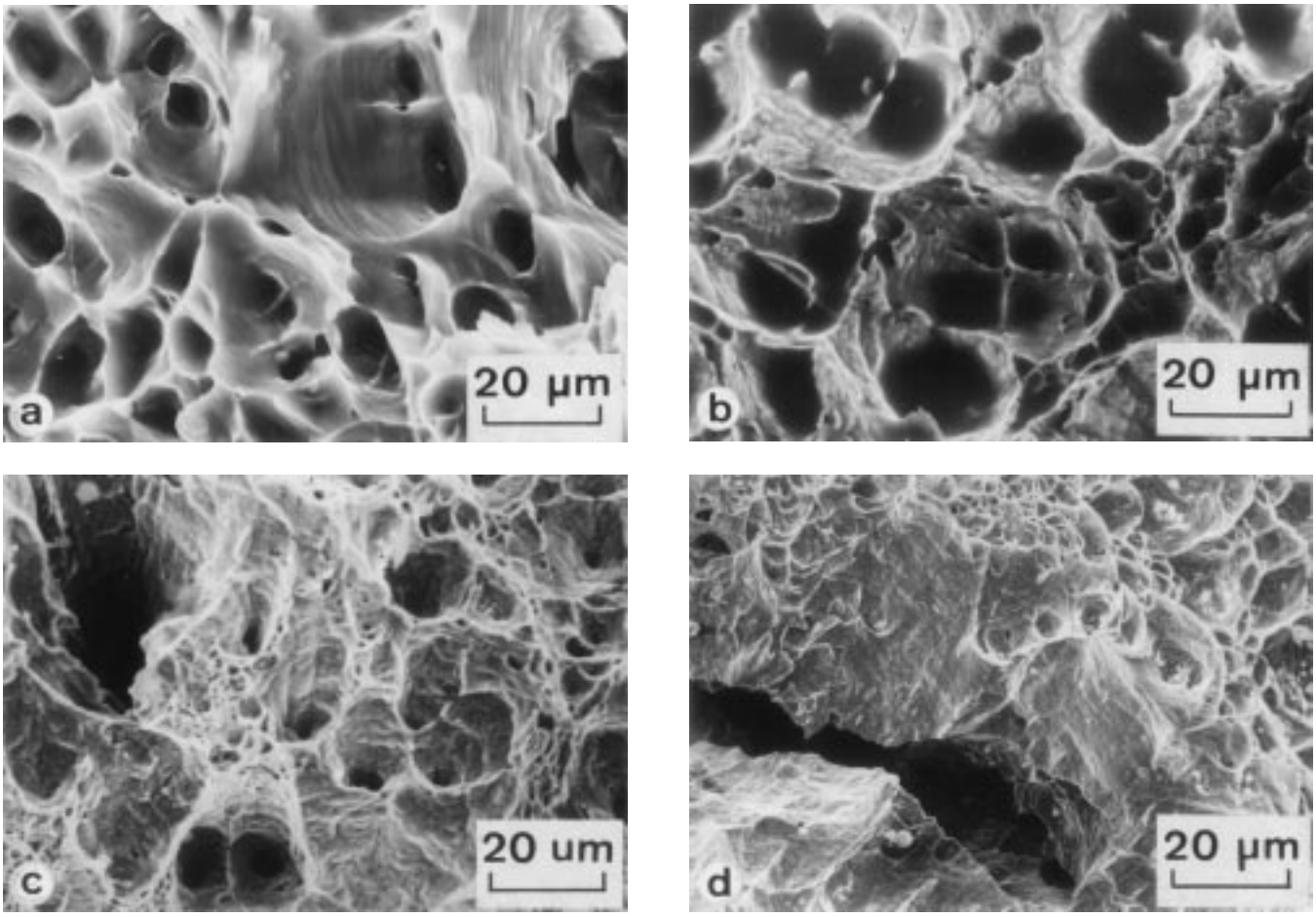

Fig. 5 Fractographs of samples. (a) The as-received condition. (b) Aged at 475 °C for 6.5 h. (c) Aged at 475 °C for 24 h. (d) Aged at 475 °C for 120 h

Table 2 Relation between time of aging and fractal dimension

Time of aging, h	Fractal dimension, *D*
0	1.19
1	1.18
2	1.15
6.5	1.11
12	1.11
24	1.10
40	1.07
120	1.05

during the fracture process. The higher the time of aging is, the smaller the size of the intervoid ligaments and the average dimple size. As a result, the surface irregularity decreases. Examples of fracture surfaces corresponding to the as-received condition and 6.5, 24, and 120 h of aging are shown in Fig. 5. For the first and second conditions (Fig. 5a, b), the larger amount of plastic growth permitted before the microvoid coalescence event is clear. On the other hand, the fracture surfaces corresponding to 24 and 120 h of aging show a mixed topography with secondary transgranular cracking as well as a dimple type of fracture mode. An expected reduction of σ_{ys} and σ_{ts} with the fractal dimension increment can be observed in Fig. 4.

The fractal approach may ultimately be perfected for adoption as a quantitative tool in fractography, but it deserves much experimental research effort.

References

1. B.B. Mandelbrot, *The Fractal Geometry of Nature*, W.H. Freeman, Ed., P.L. Renz, 1982, p 1-19
2. R.H. Dauskardt, F. Haubensak, and R.O. Ritchie, On the Interpretation of the Fractal Character of Fracture Surfaces, *Acta Metall. Mater.*, Vol 38 (No. 2), 1990, p 143-159
3. J.J. Mecholsky, Jr. and S.W. Freiman, Relationship between Fractal Geometry and Fractography, *J. Am. Ceram. Soc.*, Vol 74 (No. 12), 1991, p 3136-3138
4. J.J. Friel, A Direct Determination of Fractal Dimension of Fracture Surfaces Using Scanning Electron Microscopy and Stereoscopy, *J. Mater. Res.*, Vol 8 (No. 1), 1993, p 100-104
5. M. Tanaka, Effects of Microstructures and Creep Conditions on the Fractal Dimension of Grain Boundary Fracture in High-Temperature Creep of Heat-Resistant Alloys, *Z. Metallkd.*, Vol 84 (No. 10), 1993, p 697-701
6. B. Chiaia, A. Vervuurt, and J.G.M. Van Mier, Lattice Model Evaluation of Progressive Failure in Disordered Particle Composites, *Eng. Fract. Mech.*, Vol 57 (No. 2/3), 1997, p 301-318
7. B.B. Mandelbrot, D.E. Passoja, and A.J. Paullay, Fractal Character of Fracture Surfaces of Metals, *Nature*, Vol 308 (No. 5961), 1984, p 721-722

8. X.G. Jiang, W.Y. Chu, and C.M. Hsiao, Relationship between J_{IC} and Fractal Value of Fracture Surface of Ductile Materials, *Acta Metall. Mater.*, Vol 42 (No. 1), 1994, p 105-108
9. H. Nagahama, A Fractal Criterion for Ductile and Brittle Fracture, *J. Appl. Phys.*, Vol 75 (No. 6), 1994, p 3220-3222
10. O.A. Hilders and N.D. Pilo, On the Development of a Relation between Fractal Dimension and Impact Toughness, *Mat. Char.*, Vol 38 (No. 3), 1997, p 121-127
11. C.H. Shek, G.M. Lin, J.K.L. Lai, and Z.F. Tang, Fractal Fracture and Transformation Toughening in CuNiAl Single Crystal, *Metall. Mater. Trans.*, Vol 28A (No. 6), 1997, p 1337-1340
12. J.O. Nilsson, Super Duplex Stainless Steels, *Mat. Sci. Technol.*, Vol 8 (No. 8), 1992, p 685-700
13. L. Scoppio, and M. Barteri, Effect of Microstructure and Composition on the Mechanical Properties of Some Duplex Stainless Steels, *Applications of Stainless Steels '92*, Vol 1, H. Nordberg and J. Björklund, Ed., Jernkontoret, 1992, p 260-269
14. J. Komenda, and R. Sandström, Automatic Assessment of a Two-Phase Structure in the Duplex Stainless Steel SAF 2205, *Mater. Charact.*, Vol 31 (No. 3), 1993, p 155-165
15. J.O. Nilsson, and P. Liu, Aging at 400-600 °C of Submerged Arc Welds of 22Cr-3Mo-8Ni Duplex Stainless Steel and Its Effects on Toughness and Microstructure, *Mater. Sci. Technol.*, Vol 7 (No. 9), 1991, p 853-862
16. W. Horvath, B. Tabernig, E. Werner, and P. Uggowitzer, Microstructures and Yield Strength of Nitrogen Alloyed Super Duplex Steels, *Acta Mater.*, Vol 45 (No. 4), 1997, p 1645-1654
17. E.E. Underwood and K. Banerji, Fractal Analysis of Fracture Surfaces, *Metals Handbook.*, Vol 12, American Society for Metals, 1987, p 211-215
18. B. Dubuc, J.F. Quiniou, C.R. Carmes, C. Tricot, and S.W. Zucker, Evaluating the Fractal Dimension of Profiles, *Phys. Rev. A.*, Vol 39 (No. 3), 1989, p 1500-1512
19. B.B. Mandelbrot, *Fractals: Form, Chance and Dimension*, W.H. Freeman, Ed., 1977, p 1-32
20. E.E. Underwood and K. Banerji, Fractals in Fractography, *Mater. Sci. Eng.*, Vol 80 (No. 4), 1986, p 1-14
21. M. Nyström, B. Karlsson, and J. Wasén, The Mechanical Properties of a Duplex Stainless Steel, *Nordic Symposium on Mechanical Properties of Stainless Steels*, H. Nordberg, and K. Fernheden, Ed., Swedish Institute for Metal Research, 1990, p 70-87
22. E. Hornbogen, Fractals in Microstructure of Metals, *Int. Mater. Rev.*, Vol 34 (No. 6), 1989, p 277-296
23. X.W. Li, J.F. Tian, Y. Kang, and Z.G. Wang, Quantitative Analysis of Fracture Surface by Roughness and Fractal Method, *Scr. Metall. Mater.*, Vol 33 (No. 5), 1995, p 803-809